Hydrokinetic Energy Potential in Argentine Estuaries with High Tidal Ranges

Lucas Bindelli, Mariano Re, and Leandro D. Kazimierski

***Abstract*—Advancing in the resource assessment for the tidal stream energy harnessing is essential to have a predictable energy source. On the Patagonian coast of Argentina, there are tidal conditions with high ranges that favors the implementation of projects of this type. Specifically, there are five estuaries in which the proximity to points of energy demand transforms them into sites of interest. In this work, in these estuaries and using numerical modelling, an analysis of the hydrodynamic and energetic variables (available minimum depths, mean current velocities and potential energy) was developed, integrated with site selection indicators. The modelling strategy was based on a system of nested models to achieve greater discretization inside the estuaries (approximately 100 m and 15 s). Models were calibrated based on tidal predictions in estuarine ports due to the lack of systematic measurements. The results indicated the presence of wide areas with energy potential greater than 1.5 KW/m2 and a diversity of depths and velocities that would allow the use of different scales of energy converters.**

***Index Terms* — Tidal streams – resource assessment - Patagonian estuaries - potential energy - numerical modeling.**

I. Introduction

The extended Argentine maritime coast at the South Western Atlantic Ocean is presented as a great opportunity for marine renewable energies developments (predominantly tidal and wave energy). As a first step to advance in this line, a detailed resource assessment is required with a temporal and spatial quantification of the main variables of the system.

The southern part of the Patagonian coast presents good conditions for tidal energy harnessing due to the tidal regimes that prevail. No other areas in South America have such high tidal ranges over such a wide region [1].

In general, tidal energy harnessing is still under research and development, even though there is installed equipment that currently generates energy [2]–[4]. The predictability of this source is one of the great advantages compared to other renewable energy sources.

Tidal stream energy, also known as hydrokinetic energy, is related to the constant movement of the tidal flow. Energy conversion is made through one or more turbines that are installed underwater at high velocity locations. This way of energy harness is similar for wind turbines, though, given the higher density of water compared to that of the air, a lower rotation speed and with a lower span area a hydrokinetic turbine can produce the same amount of energy (this is a relative advantage over wind power).

L. Bindelli, M. Re and L. Kazimierski are part of the Instituto Nacional del Agua, Laboratorio de Hidráulica, Ezeiza, Argentina, and Universidad de Buenos Aires, Facultad de Ingeniería, Buenos Aires, Argentina (e-mails: lucasbindelli@gmail.com, m.re@ina.gob.ar & leandrokaz@gmail.com).

Estuarine areas are ideal locations for hydrokinetic energy harness due to their morphology. This condition, added to the occurrence of high tidal ranges, is an opportunity to take advantage of that energy in nearby high-consumption sites such as cities or ports. Interest in studying the tidal energy potential of estuaries is growing [5]–[8].

In Argentina, the estuaries of Southern Patagonia (Fig. 1) present high tidal ranges [9] and favorable conditions for a tidal stream harnessing. According to [1], Rio Grande (GrRE), Rio Gallegos (GaRE), Rio Coyle (CoRE) and Rio Santa Cruz (SCRE) estuaries are hypertidal and Rio Deseado (DeRE) is macrotidal. Tide is semidiurnal in all cases, with mean amplitudes ranging between 4 and 9 *m*.

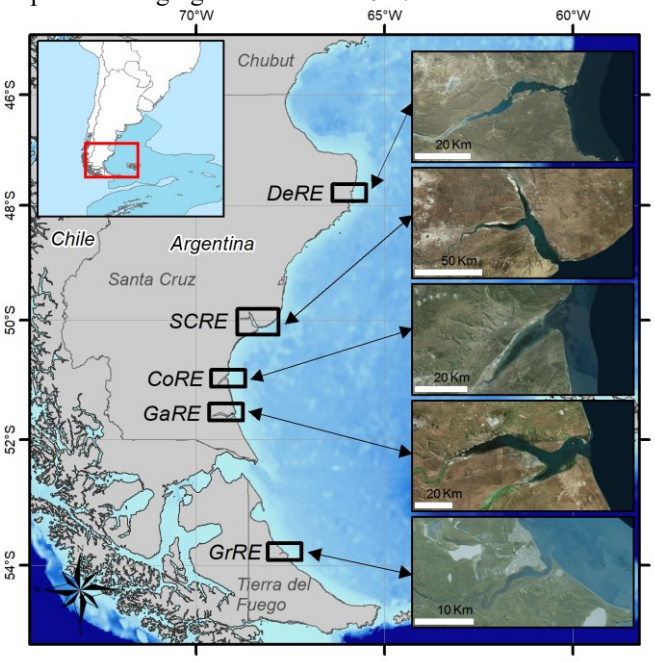

Fig. 1. Patagonian estuaries. Santa Cruz and Tierra del Fuego provinces, Argentina.

In this paper, the hydrokinetic energy potential was assessed in five Argentine estuaries with high tidal ranges located in Southern Patagonia. A comparative analysis of the main variables and site location indicators was developed to characterize the tidal current resource through numerical modeling. The main goal of this work is to characterize in detail this strategic resource that, considering the development of new harnessing technologies, could become a competitive energy source in the near future.

II. Methodology

The base of the methodology used in this analysis consists of hydrodynamic simulations by means of the software Delft3D [10]. The Delft3D-FLOW module is a finite difference code that solves the Navier-Stokes equations for an incompressible fluid into two (depth-averaged) or three dimensions under shallow water, Boussinesq approximations. This modelling approach uses the 2D-H approximation, which consists of the resolution of the horizontal momentum equation, the continuity equation, and a turbulence closure model. Only the astronomical tide was modeled (in this area the effect of the meteorological tide is negligible in comparison). River discharges were not considered since the dynamics of estuaries are governed almost entirely by the astronomical tide [11]. To achieve statistically significant results, the simulations contemplated a period of one year (2017).

The modelling strategy was addressed using nested models [12]. This implies the implementation of a regional model for the Southwestern Atlantic Ocean / Argentine Sea, named Rank 0, with an extension adequate to represent the Argentinean Continental Shelf circulation. This model was forced by the astronomical tide using 13 tidal components (M_2, S_2, N_2, K_2, $2N_2$, K_1, O_1, P_1, Q_1, M_1, M_f, M_m and M_{sqm}) obtained from the global model FES-Global Tide 2014b [13]. Then, a second model (Rank 1) related to the Argentinean Continental Shelf was proposed and nested to the Rank 0 (Fig. 2). This model includes all the five selected estuaries. To achieve a discretization of detail within each estuary (in the order of 100 *m* and 15 *s*), the nesting of two more models for each estuary was implemented (Ranks 2 and 3).

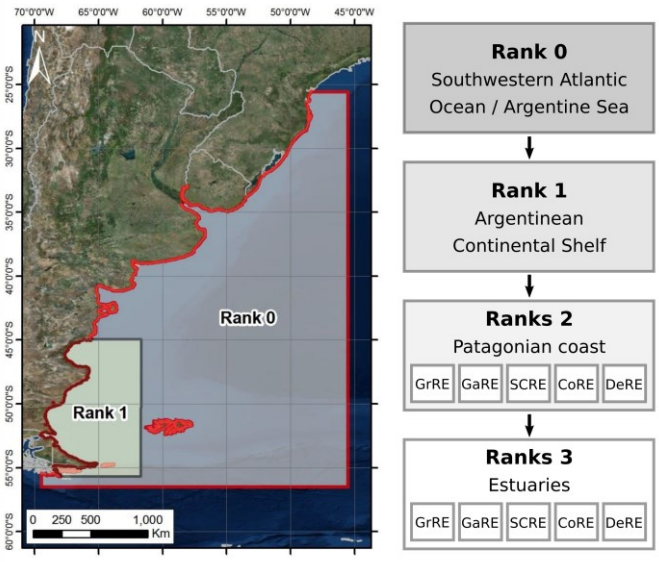

Fig. 2. Nested models. Numerical modelling domains.

The model's bathymetry was built using the global model GEBCO (General Bathymetric Chart of the Oceans) [14] based on a grid resolution of 30'. Nearshore global data is inaccurate, therefore nautical charts of the Argentine Hydrographic Service (SHN) were used. Inside the estuaries this data is also insufficient, so satellite images and tidal levels were used to delimit the coastline [15].

Due to the lack of observations in these estuaries, the modelled water level series were compared to the predicted astronomical tide series estimated by the SHN at the main ports of the zone. The performance of the simulations was evaluated using two indicators: *i)* root mean square of error (RMSE), and *ii)* coefficient of determination (R^2).

The modeling system calibration was performed using the bottom roughness coefficient (Manning's "n" value). The adopted coefficient was 0.015 for all the Ranks, due to the better fitting of the general dynamics. TABLE I shows the values of the error indicators corresponding to the detailed models of each estuary (Rank 3). It is considered that results of this quality, in estuaries without systematic observations and with large tidal ranges, are adequate to have a first approach of the availability of the resource.

TABLE I
PERFORMANCE INDICATORS – RANK 3 MODELS

Estuary	RMSE [*m*]	R^2
DeRE	0.32	0.96
SCRE	0.57	0.96
CoRE	0.83	0.93
GaRE	0.77	0.94
GrRE	0.46	0.95
Mean (five estuaries)	0.62	0.95

Once the hydrodynamics of each estuary have been solved, the energy potential can be obtained based on the simulated depths and current velocities. Equation (1) links the flow velocities that occur during a certain amount of time and at a specific cross-sectional area, with the energy potential contained in that flow.

$$\frac{P}{A}(x,y) = \frac{1}{2} \cdot \rho \cdot |V(x,y)|^3 \qquad (1)$$

Where P is the available energy potential in terms of power in *kW*, A is the cross section of each cell of the computational grid in m^2, ρ is the water density in kg/m^3, and V(x,y) is the average velocity of each cell of the computational grid in *m/s*.

For the hydrodynamic and energetic characterization, three variables were identified that explain the availability of the resource in each estuary: i) minimum depths (MiD), ii) depth-averaged mean current velocities (MCV), and iii) depth-averaged mean power density (MPD). Then, to integrate these results and specify the best locations of each estuary, three indicators that correspond to the state of the art of this type of analysis were evaluated: TSE_{ndl} (non-depth-limited Tidal Stream Exploitability index) [8], IHE (Integrated Hydrokinetic Energy index) [16] and NREL (NREL Score) [17].

Due to the high tidal range of the area, it was necessary to analyze the MiDs reached in each case. Hydrokinetic turbines need to be always fully submerged during the generation, with a top margin from the water surface to avoid deficiencies in their performance [18] and a bottom margin to avoid any type of erosion [19]. For this analysis, minimum depths were divided into two groups regarding the conversion technology to be used: *i)* < 20 *m*: prototypes and small-scale devices, and *ii)* ≥ 20 *m*: large-scale devices.

Due to instantaneous velocity maximums only occur during

very short periods, a more accurate characterization was employed for the MCVs definition. Only MCVs ≥ 1 *m/s* are considered relevant, since this is the cut-in speed for most mid to large scale converters. For this, modulus velocity values were used, considering both flood and ebb tides as equally relevant.

Likewise, maximum instantaneous power density is deprecated and only MPD is considered relevant. In this case, MPD ≥ 0.5 kW/m^2 are analyzed, which is the result of replacing the MCV threshold in (1). Then, based on the established thresholds for depth and power, results are condensed into delimitation maps that allow an assessment of the resource, including its flexibility and limitations.

The three chosen indexes cover different approaches of site selection, the TSEndl being an index that only considers depths and maximum velocities, while IHE index and NREL Score cover other technical parameters involved in hydrokinetic energy harnessing, such as distance to shore, or market size. These indexes are explained next, specifying the adopted values and the references for the involved parameters.

TSE index was designed for site selection in areas with limited water depth [20] and later modified by [8] for non-depth-limited cases (TSEndl). Index values above 1 indicate suitability for exploitation (the higher, the better) and are obtained applying (2).

$$TSE_{ndl} = \frac{\xi_{ndl}}{2V_0{}^3 h_0}\left(V_f^3 + V_e^3\right)h \qquad (2)$$

where V_0 and h_0 represent the characteristic velocity and water depth, respectively, which are usually set as 1.5 m/s (V_0) and 5 m (h_0); V_f and V_e are the average velocities at mid-flood and mid-ebb, respectively; h is the water depth at mid-tide and ξ_{ndl} is a penalty function which depends on the water depth and adopts maximum values between 12 and 22 m.

The IHE index takes a holistic approach by integrating three main aspects affecting the installation of hydrokinetic energy farms: *(i)* the exploitable resource, considering current velocities within cut-in and cut-out values; *(ii)* the geomorphological configuration, for which the main Capital Expenditures (CAPEX) of a hydrokinetic farm are parameterized according to water depth and shoreline distance; *(iii)* the socioeconomic activities and environmental uses which are considered by analyzing and parameterizing geospatial data. Index values above 1 indicate suitability for exploitation (the higher, the better) and are obtained applying (3).

$$IHE = HE * C_{gp} * U_{gp} \qquad (3)$$

where HE is the hydrokinetic energy resource index [item *(i)*], according to which values equal to or higher than 1 indicate suitability for energy exploitation; C_{gp} is a geospatial cost penalty function (values ranging from 0 to 1) [item *(ii)*], meaning that a location with C_{gp} = 1 is not penalized by the costs that are associated to the operation and maintenance of a hydrokinetic farm, and where C_{gp} = 0 has the largest penalization (in the latter case, IHE = 0); and U_{gp} stands for the geospatial water use penalty function (values ranging from 0 to 1) [item *(iii)*], having the same interpretation as C_{gp}.

Distance to shoreline was measured from geospatial maps and, even though there are no interfering environmental uses in any of the selected estuaries, a value of U_{gp} = 0.9 was adopted in consideration for possible environmental uses in the future.

For the NREL Score, a Multi-Criteria Decision Analysis framework was used to create a composite score and generate rankings of tidal sites in USA. This score is obtained from:

$$S = \prod_i s_i^{w_i} = S_p \cdot S_m \cdot S_{dist} \cdot S_d \qquad (4)$$

where s_i and w_i are the partial scores and relative weights, respectively, for each of the criteria. Total composite score for a site, S, is between 0 and 10, with weights normalized such that, $\Sigma_i w_i$=1 and equally distributed (w_i=1/5 ∀i).

These composite scores are used to rank sites in terms of their suitability for early tidal technology deployment. Resource density (S_p) and market size (S_m) criteria are indicators for the technical and commercial viability of a project. Higher resource density and larger markets are likely to be more attractive to project developers, and these criteria are therefore scored positively. Shipping costs and distance to resource (S_{dist}), and water depth (S_d) criteria are indicators for total project cost. Sites with larger costs are considered less attractive, and these criteria are therefore scored negatively. In this case, only the long-term version of this index was calculated, not including the energy price's partial score, to obtain results that are less dependent on external factors. Amplitudes and tidal volume fluxes were obtained from numerical simulations. Power grid distances were measured from geospatial maps. Transportation costs were established considering a negative ponderation for large distances based on [17].

III. RESULTS

Following the procedure described in II, the results of the main hydrodynamic and energetic characteristics of each estuary obtained from the detail models are analyzed.

Geographical MiD distributions are shown in Fig. 3 a-e. For DeRE only MiDs < 20 *m* are found (the deepest along the river channel and estuary's mouth), for both CoRE and GrRE only MiDs < 5 *m* are present, and for SCRE and GaRE, MiDs > 20 m are present, with the deepest areas located mainly at the estuary's mouth in both cases.

Regarding the results of MCV, and as an example, Fig. 4 presents the results for SCRE, where the 1 *m/s* threshold is exceeded between the estuary's mouth and Punta Quilla, 4 *km* inland. The sub-plots show the distribution of instantaneous velocity by means of a probability density function and a box-plot chart in points of different MCV values, justifying the use of MCV rather than maximum velocities. Similar results were obtained in all cases, exceeding MCV threshold both during flood and ebb tides.

As for the other cases, at DeRE, MCV values exceeding the threshold are located between the estuary mouth and up to 13 *km* inland. At CoRE, values over the threshold are located at the estuary mouth and 10 *km* inland near the Southern margin. At GaRE, MCV exceeds 1 *m/s* throughout almost the entire estuary's length and up to 20 *km* inland from the mouth. And at GrRE, threshold surpassing MCVs are present at the river

mouth, in coincidence with the central channel of the river, forming an elongated area of 5 *km* in length.

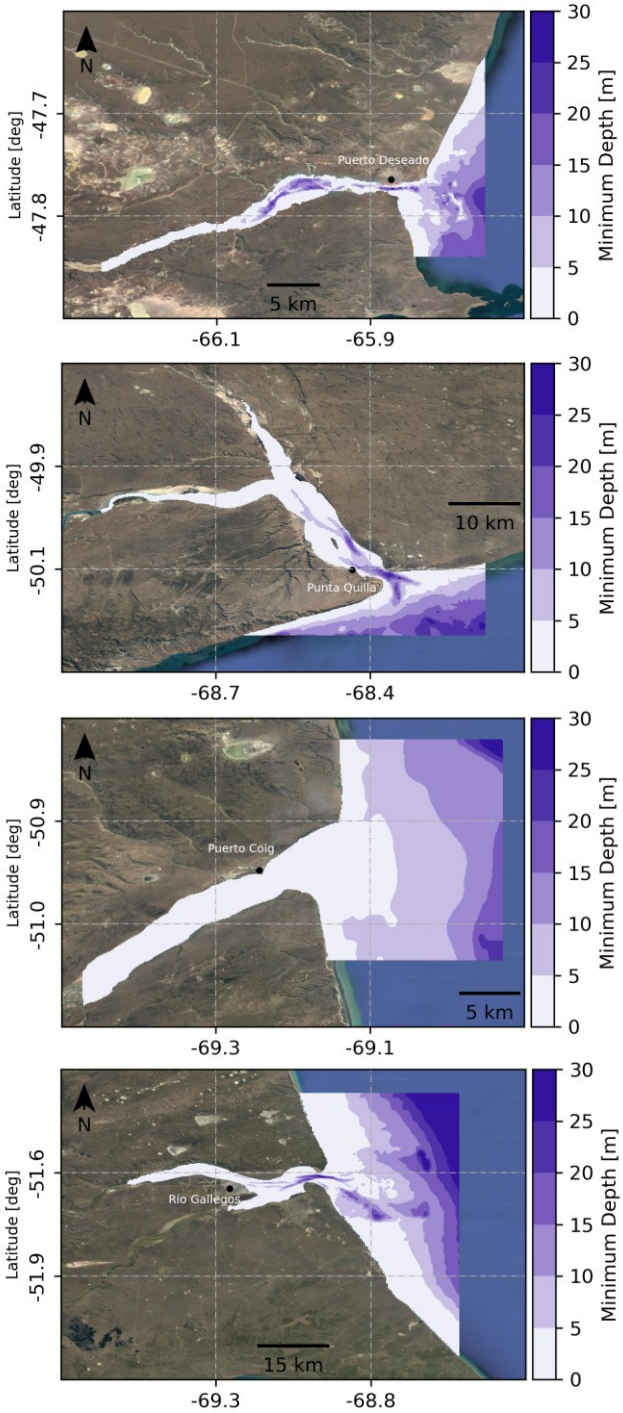

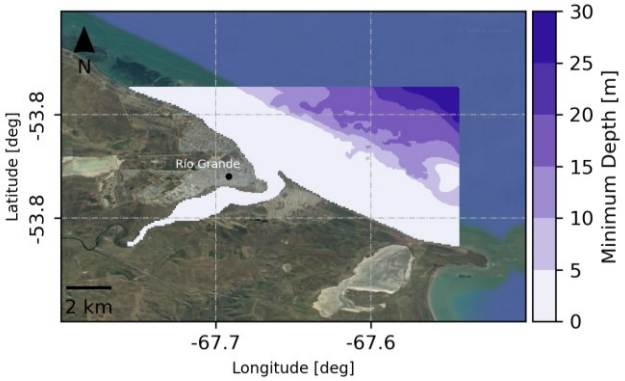

Fig. 3. Minimum Depth (MiD) for: a. DeRE, b. SCRE, c. CoRE, d. GaRE, e. GrRE.

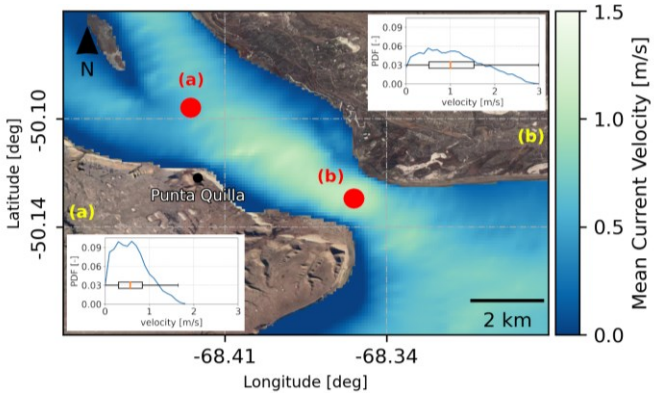

Fig. 4. Mean Current Velocities (MCV) and PDF distributions for SCRE.

Applying (1) for each estuary, the results for MPD were obtained and are shown in Fig. 5. In all five estuaries significant areas with MCD values exceeding 1.5 kW/m^2 are found, following an identical distribution to that described for MCVs.

Due to areas of high MCV (≥ 1 *m/s*) and MPD (≥ 0.5 kW/m^2) don't necessarily coincide with those of highest MiD within each estuary, a histogram was obtained to establish the area distribution of high MCV with MiD (Fig. 6-a). Summarizing, DeRE contains 252 *Ha* of interest, but none has a MiD of over 20 m; SCRE has 233 *Ha* of interest, with 21 of them presenting MiDs $\geq$ 20 m; CoRE has 146 *Ha* of interest, with no area with MiDs over 20 *m*; GaRE has 8272 *Ha* of interest, from which 354 *Ha* have MiDs $\geq$ 20 *m*; GrRE has 32 *Ha* of interest, all of them under 20 *m* of MiD.

On the other hand, it is also valuable for the comparison to establish the distribution of areas surpassing the MCV threshold by ranges of MPD (Fig. 6-b), where relevant aspects for each estuary can be named: for DeRE there is an even distribution ranging around 40 *Ha* in this case. Maximum area is of about 85 *Ha* at an MPD of over 1 kW/m^2, whereas for the category of over 2.5 kW/m^2 of MPD, there are 45 *Ha* available. For SCRE, all its high MPD area (233 *Ha*) corresponds to the 1 to 2 kW/m^2 range, from which 5 *Ha* are higher than 1.5 kW/m^2. For CoRE, there is an even area distribution between all the ADP categories, ranging around 20 *Ha*, except for the 67 *Ha* at MPD of over 1 kW/m^2. For the highest category of over 2.5 kW/m^2 there is an area of 24 *Ha*. For GaRE, available areas range from over 1000 to almost 3000 *Ha* for the range of 1 to over 2.5 kW/m^2 with a maximum of 2840 *Ha* for the highest category. Also, for MPD of over 0.5 *kW/m2*, there is an area of 243 *Ha*.

For GrRE, available areas with high MPD range around 10 *Ha* between 1 and 2 kW/m^2, with 6 *Ha* for an MPD of over 2 kW/m^2.

Condensing these results and considering the thresholds for MiD and MPD, 4 categories can be delimited: small-scale devices (MiDs < 20 *m*), large-scale devices (MiDs ≥ 20 *m*), testing areas ($0.5 \leq MPD \leq 1$ kW/m^2), and operating areas (MPD ≥ 1 kW/m^2) generating 4 areas of interest: for testing small-scale devices (S-T), for operating small-scale devices (S-O), for testing large-scale devices (L-T) and for operating large-scale devices (L-O). The distinction between testing and operating is considered useful for the developing stages of the harnessing, needing more controlled conditions in such cases. TABLE II presents a summary of the areas obtained from the delimitation maps, such as the one shown for GaRE (Fig. 7).

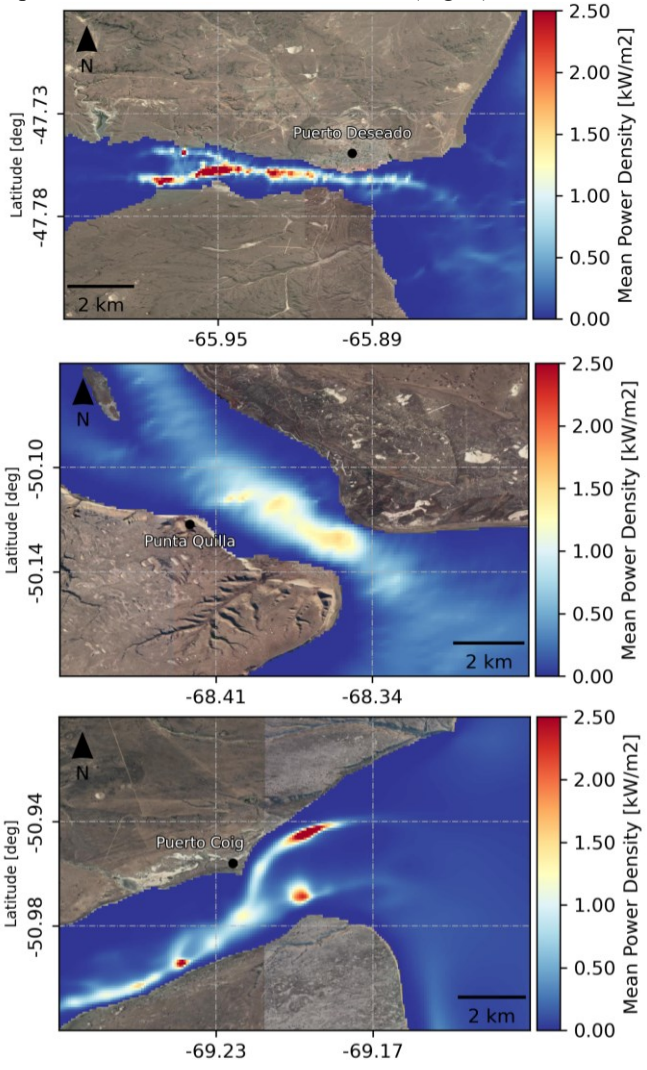

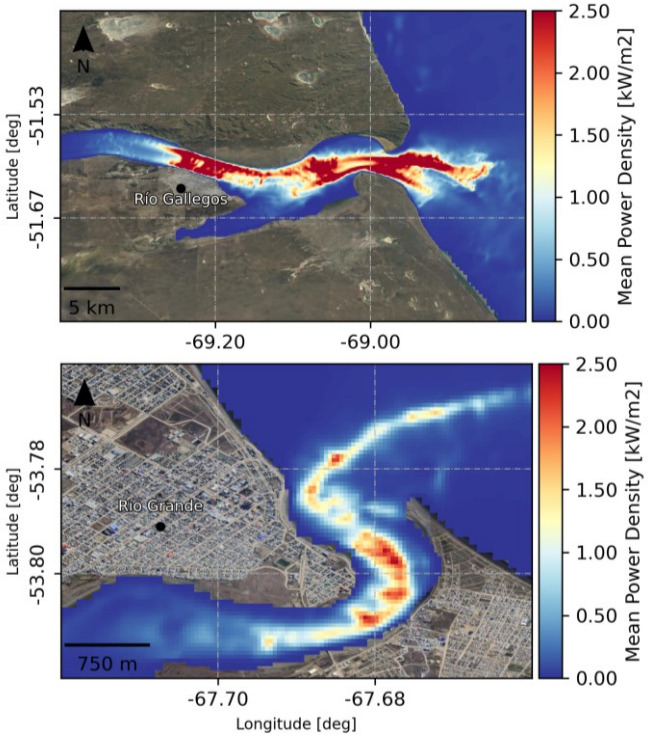

Fig. 5. Mean Power Density (MPD) for: a. DeRE, b. SCRE, c. CoRE, d. GaRE, e. GrRE.

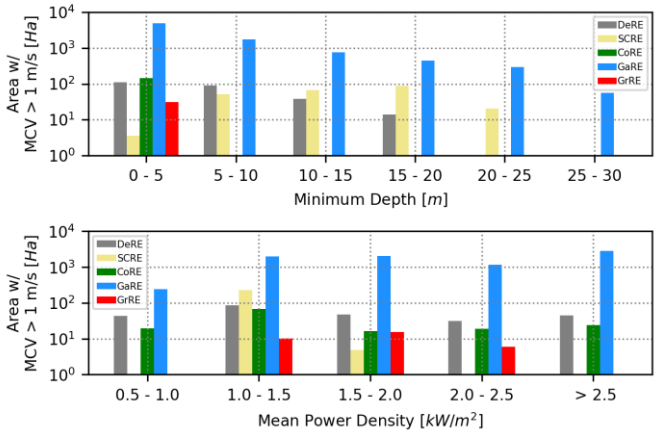

Fig. 6. Distribution of high MCV by MiD (a) and by MPD (b) for: a. DeRE, b. SCRE, c. CoRE, d. GaRE, e. GrRE.

TABLE II
DELIMITATION MAPS RESULTS

Estuary	Area for S-T [*Ha*]	Area for S-O [*Ha*]	Area for L-T [*Ha*]	Area for L-O [*Ha*]
DeRE	689	217	5	-
SCRE	754	355	62	32
CoRE	631	238	-	-
GaRE	3272	8302	-	354
GrRE	77	72	-	-

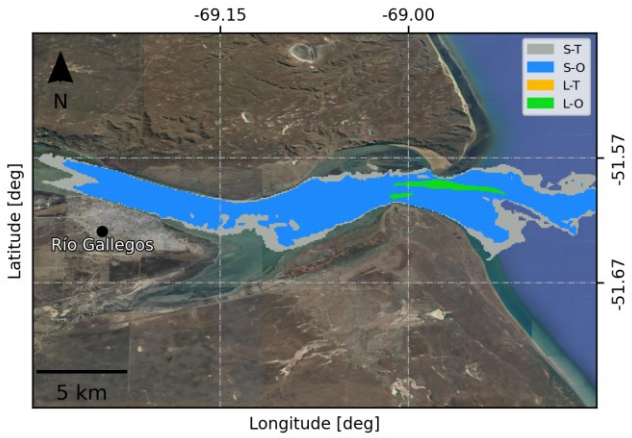

Fig. 7. Delimitation of areas of interest for GaRE.

Regarding the three selected indexes, results are summarized in TABLE III, where areas of interest are shown for TSE_{ndl} and IHE, and the Score for NREL is shown (no threshold is defined in this case, only the score, for relative comparison).

TABLE III
SITE CHARACTERIZATION INDEXES RESULTS

Estuary	Area with TSE > 1 [*Ha*]	Area with IHE > 1 [*Ha*]	NREL Scores
DeRE	284	1192	6.0
SCRE	2380	1050	7.7
CoRE	-	1359	-
GaRE	4185	9421	6.8
GrRE	-	240	4.0

IV. Discussion

According to [6], site selection for tidal stream exploitation projects is based on two criteria: great depths and high velocities. Reference [21] suggested water depths in a range between 25 and 50 *m*, and current velocities greater than 2.5 *m/s* during spring tides. These aren't common values in estuaries and near points of energy demand. As for power density, depth-averaged mean values of 5 to 7.5 kW/m^2 can be found in high energetic areas of hypertidal estuaries [6],[7].

A detailed analysis of the three variables of interest in each of the Argentine estuaries studied allows us to assert that the availability of the resource is different in all of them. MiD values over the 20 *m* threshold can only be found in two of the estuaries (SCRE and GaRE), whereas only the latter meets the criteria established by [21] (MiD ≥ 25 *m*). Regarding the other three estuaries, DeRE presents appealing characteristics, with values of over 15 *m*, while CoRe and GrRE only have MiDs below 5 *m*, limiting their aptitude to small scale harnessing, like in [5]. On the other hand, MCV values higher than 1 *m/s* are met in all five estuaries, but in different extents, ranging from a few (GrRE) to thousands (GaRE) of hectares. During the simulations, peak (instantaneous) values of 2.5 *m/s* are reached in the five cases. Such values can be found in river harnessing locations as described in [8]. Though below expected values for hypertidal locations, Fig. 4 deprecates utilising maximum velocities as a reference for being misleading towards overestimation. An example of this is the case presented by [7], where peak values reach 3 m/s, while mean values are under 2 *m/s*. The assessment of high velocity areas through the MCV variable seeks to establish a more robust characterization. In terms of MPD, all but SCRE have an even distribution of surface availability in the range of 0.5 – 2.5 kW/m^2. For SCRE, only values between 1.0 and 2.0 kW/m^2 are found. Even though these values are about half of those described by [6] and [7], they are still significant values, exceeding those estimated for micro and meso-tidal regimes [5], [8], [22]. These five estuaries could therefore be considered as mid-scale tidal stream harnessing locations.

Even though results obtained for TSE_{ndl}, IHE and NREL were generally favorable, different aspects can be discussed. TSE_{ndl} results are positive for DeRE, SCRE and GaRE, but are misleading in terms of the present work, for only considering peak velocities. Also, depth penalization (> 22 m) is not in line with the dimensions of current turbine developments [23]. IHE results present large areas of interest. Even though it is a more robust index by considering multiple key factors, it measures MPD from a rather low reference value (0.2 kW/m^2). Plus, many coefficients need to be obtained, not necessarily maintaining representativity in their calculation, since assumptions need to be made beforehand. NREL results are favorable in all but CoRE (due to large distances from the power grid), placing the rest of the estuaries in positions 12° (SCRE), 19° (GaRE), 21° (DeRE) and 35° (GrRE) out of the 36 best locations in all USA for hydrokinetic harnessing. This index follows a similar approach to IHE, with a more accurate threshold for MPD (0.5 kW/m^2), but the result is a score that only provides information relative to other sites of interest, and not of the site itself.

Having different weak-spots and reaching to different results for the same estuary (Fig. 8), neither of these indexes stands out above the others. On the other hand, delimitating areas depending on final use seems a simpler and more direct approach for a fist assessment, since the only variables needed are MiD and MPD, with the sole arbitrary aspect being the established thresholds in each case. Here, results show different applications: DeRE, CoRE and GrRE are suitable for testing and operating small-scale devices, while SCRE and GaRE are suitable for operating small and large-scale devices, recommending only SCRE for testing large-scale devices.

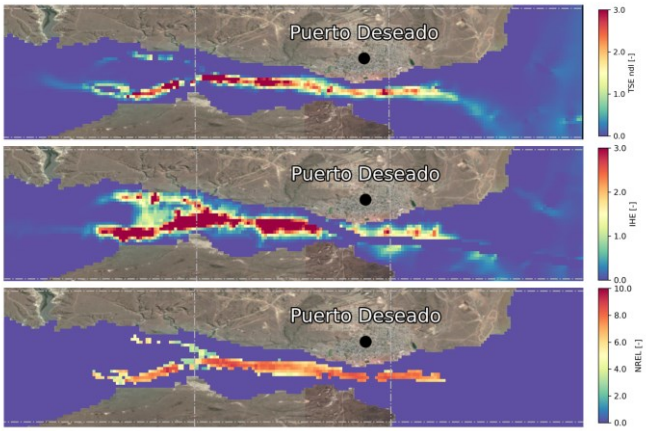

Fig. 8. Comparison between TSE_{ndl}(a), IHE (b) and NREL(c) indexes for DeRE.

Besides flexibility, other advantages of these estuaries are the bidirectionality of the flow, allowing for use of reversible flow turbines, and the fact that almost all the high MPD found is located inside the estuaries. This results in protected locations

that become less susceptible to strong weather events that could damage the equipment [24], [25], but also restricting directionality of the flow, which produces currents with little variation in direction.

As closure for this section, SCRE and GaRE present themselves as the best two of the five estuaries regarding tidal stream harnessing, due to the relatively good MiDs, high MCV and MPD inside the estuaries, as well as at relatively good width, which is ideal for limiting interferences with other water uses of the estuaries.

V. Conclusions

The first comprehensive hydrodynamic and energetic study of five estuaries in southern Argentina with high tidal ranges was conducted. It was important to use the same methodology in the five sites to favor comparisons of their characteristics linked to the use of tidal stream energy.

The models performance resulted satisfactory; error indicators remained bounded at permissible values. The main limitation of this methodology is the validation of the generated models. The realization of velocity and bathymetric surveys would improve their implementation, and the results of this work could be used to select the areas of interest.

In all the five estuaries selected high velocities due to tidal currents were obtained, both during flow and ebb tides. The bidirectionality of tidal flows would allow the hydrokinetic energy harnessing at the two stages of the flow using the appropriate turbines.

The indexes found in the literature, though useful, present different outcomes depending on many factors that prevent straightforward conclusions and comparisons between sites.

The available energy potential, although it is not one of the largest in the world, is high. The alternative offered by these Argentine estuaries is that the areas of high potential are very extensive. The possibility of scaling this type of exploitation is one of the distinctive characteristics of this region.

In summary, the five estuaries present harnessable energy potential. The technology to be used in each one would probably vary given the differences in depths and velocities available.

Acknowledgment

The authors would like to thank de National Water Institute authorities (INA, Argentina) for providing the facilities, and to the CONICET and the YPF Foundation for funding.

References

[1] A. W. Archer, “World's highest tides: Hypertidal coastal systems in North America, South America and Europe”, Sedimentary Geology, vol. 284–285, pp. 1-25, Feb 2013. DOI: 10.1016/J.SEDGEO.2012.12.007

[2] I. M. Yuce, A. Muratoglu, “Hydrokinetic energy conversion systems: A technology status review”, *Ren. and Sust. Energy Reviews*, vol. 43, pp. 72-82, March 2015.

[3] C. M. Niebuhr, “A review of hydrokinetic turbines and enhancement techniques for canal installations: Technology, applicability and potential”, *Ren. and Sust. Energy Reviews*, vol. 113, 109240, Oct. 2019.

[4] M. S. Chowdhury,. “Current trends and prospects of tidal energy technology”, *Environ Dev Sustain, vol.* 23, pp. 8179–8194, June 2021. https://doi.org/10.1007/s10668-020-01013-4

[5] N. D. Badano, R. Espina Valdés, E. Álvarez Álvarez, “Tidal current energy potential of Nalón river estuary assessment using a high precision flow model”, Open Eng., vol 8, pp. 118–123, May 2018. https://doi.org/10.1515/eng-2018-0015.

[6] A. Mohammadian, B. Morse, J. L. Robert, “Assessment of Tidal Stream Energy resources in a hypertidal estuary with highly irregular bathymetry using 3D numerical modelling”, *J. Ocean Eng. Mar. Energy*, vol. 5, pp. 267–281, July 2019. https://doi.org/10.1007/s40722-019-00138-7

[7] T. Wang, Z. A. Yang, “Tidal Hydrodynamic Model for Cook Inlet, Alaska, to Support Tidal Energy Resource Characterization”, J. Mar. Sci. Eng., vol. 8, no. 4, 254, April 2020. https://doi.org/10.3390/jmse8040254.

[8] D.M. Fouz, R. Carballo, I. López, G. Iglesias, “Tidal Stream Energy potential in the Shannon Estuary”, *Renewable Energy*, vol. 185, pp. 61-74, Feb. 2022.

[9] M. C. Piccolo and G. M. E. Perillo, “Estuaries of Argentina: A review” in *Estuaries of South America: Their geomorphology and dynamics*, ed. G.M.E. Perillo, M.C. Piccolo, and M. Pino Quivira, Berlin: Springer, 1999, ch. 6, pp. 101–132.

[10] Deltares, “*Delft3D-FLOW User Manual*”, *Deltares*, 2013, Delft, The Netherlands, vol. 330.

[11] M. G. Dinápoli, J. J. Ruiz, C. G. Simionato, G. Berden, “Improving the short-range forecast of storm surges in the Southern-West Atlantic Continental Shelf using 4DEnSRF data assimilation”, *Quarterly Journal of the Royal Met. Soc., to be published.*

[12] L. Bindelli, L. D. Kazimierski, M. Re, “Evaluación del potencial energético de las corrientes de marea en estuarios patagónicos mediante modelación numérica. Informe II – Modelos numéricos y potencial energético”, *National Water Institute, Buenos Aires, Argentina*, 2020.

[13] F. H. Lyard, “FES2014 global ocean tide atlas: design and performance”, Ocean Sci., vol. 17, no. 3, pp. 615–649, May 2021. https://doi.org/10.5194/os-17-615-2021.

[14] P. Weatherall, “A new digital bathymetric model of the world's oceans”, Earth and Space Science, vol. 2, no. 8, pp. 331–345, Aug. 2015. doi:10.1002/2015EA000107.

[15] F. Haspert (2018). Delimitación de la zona intermareal de cinco estuarios patagónicos mediante el uso de imágenes satelitales. Presented at IFRH - 4th. Meeting of Young Researchers in Water Resources, Argentina.

[16] D.M. Fouz, R. Carballo, I. López, G. Iglesias, “A holistic methodology for hydrokinetic energy site selection”, *Appl. Energy*, vol. 317, Apr. 2022.

[17] L. Kilcher, "Early Market Opportunity MHK Energy Site Identification - Wave and Tidal Resources", Apr. 2016. https://dx.doi.org/10.15473/1439876.

[18] A. S. Bahaj, A. F. Mollando, J. R. Chaplin, W. M. J. Batten, “Power and thrust measurements of marine current turbines under various hydrodynamic flow conditions in a cavitation tunnel and a towing tank”, *Renewable Energy*, vol 32, no. 3, pp. 407-426, March 2007. https://doi.org/10.1016/j.renene.2006.01.012

[19] C. Hill, M. Musa, M. Guala, “Interaction between axial flow hydrokinetic tubrines and uni-directional flow bedforms”, *Renewable Energy*, vol. 86, pp. 409-421, Feb. 2016.

[20] G. Iglesias, M. Sánchez, R. Carballo, H. Fernández, “The TSE index – A new tool for selecting tidal stream sites in depth-limited regions”, *Ren. Energy*, vol. 48, pp. 350-357, June. 2012.

[21] A. S. Iyer, *et al.*, “Variability and phasing of tidal current energy around the United Kingdom”, *Renewable Energy*, vol. 51, pp. 343–357, March 2013.

[22] I. Iglesias, A. Bio, L. Bastos, P. Avilez-Valente, “Estuarine hydrodynamic patterns and hydrokinetic energy production: The Douro estuary case study”, *Energy, vol*. 222, 119972, May 2021.

[23] T.R. Munaweera Thanthirige, J. Goggins, M. Flanagan, W. Finnegan, “A State-of-the-Art Review of Structural Testing of Tidal Turbine Blades”. *Energies,* vol. 16, 4061, May 2023. https://doi.org/10.3390/en16104061

[24] D. Kumar, S. Sarkar, “A review on the technology, performance, design optimization, reliability, techno-economics and environmental impacts of hydrokinetic energy conversion systems”, *Renewable and Sustainable Energy Reviews*, vol. 58, pp. 796-813, May 2016.

[25] S. Walker, P.R. Thies, “A review of component and system reliability in tidal turbine deployments”, *Ren. and Sust. Energy Reviews*, vol. 151, 111495, Nov. 2021.

Lucas Bindelli has a degree in Civil Engineering from Facultad de Ingeniería at Universidad de Buenos Aires (UBA), in 2018, and currently is doing a PhD in Engineering at UBA. His main interests are related to the analysis of the hydrodynamic performance of hydrokinetic turbines in water bodies with high energy potential.

Mariano Re has a degree in Civil Engineering from Facultad de Ingeniería at Universidad de Buenos Aires (UBA), in 2000, a Master's degree in Environmental Sciences from Facultad de Ciencias Exactas y Naturales at UBA, in 2005. He is currently a professor at the Engineering graduate program in Numerical Modelling at UBA and is the Head of Computational Hydraulics Program at Hydraulics Laboratory (INA, National Water Institute).

Leandro D. Kazimierski has a degree in Civil Engineering from Facultad de Ingeniería at Universidad de Buenos Aires (UBA), in 2014, and is student at the master's degree in Management and Planning of Urban Engineering from Facultad de Ingeniería at UBA. He is currently an assistant professor at the Engineering graduate program in River Hydraulics and Hydraulic Models at UBA and is the Head of River Hydraulics Program at Hydraulics Laboratory (INA, National Water Institute).